

Electronic Supplementary Information

**In situ and sensitive monitoring of configuration-switching involved
dynamic adsorption by surface plasmon-coupled directional enhanced
Raman scattering**

Xiao-Hui Pan ^a, Shuo-Hui Cao ^{a,b}, Min Chen ^a, Yan-Yun Zhai ^a, Zi-Qian Xu ^a, Bin Ren ^{a,c}, Yao-Qun Li ^{*a}

^a *Department of Chemistry and the MOE Key Laboratory of Spectrochemical Analysis & Instrumentation, College of Chemistry and Chemical Engineering, Xiamen University, Xiamen 361005, China*

^b *Department of Electronic Science, Xiamen University, Xiamen 361005, China*

^c *State Key Laboratory of Physical Chemistry of Solid Surfaces, College of Chemistry and Chemical Engineering, Innovation Center of Chemistry for Energy Materials, Xiamen University, Xiamen 361005, China*

* *Corresponding Author. E-mail address: yaoqunli@xmu.edu.cn*

1. Chemicals and reagents

Malachite Green (99 %) was purchased from Tianjin Beilian Fine Chemicals Development Co., Ltd.

Trisodium citrate (99 %), chloroauric acid (99 %), and glycerol (99 %) were obtained from Sinopharm Chemical Reagent Co., Ltd. All chemicals were used as received. Ultrapure water was used to prepare all aqueous solutions.

2. The SPCR instrumental setup

Fig. S1 shows the experimental setup for RK-SPCR and the conventional SERS detection.

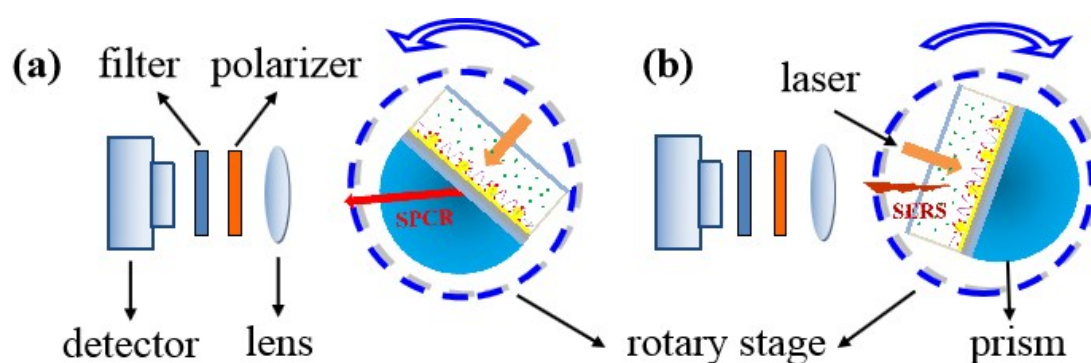


Fig. S1 The scheme of collection methods of (a) the SPCR emission on the prism side and (b) the conventional SERS on the sample side passed through a lens, a rotatable polarizer, a long-pass filter and were then collected by a spectrometer.

3. Simulations

Table S1 The simulated parameters of surface plasmon resonance curve of malachite green.

Layer	Composition	Thickness/nm	Refractive index	Extinction coefficient
1	BK7	0	1.51	0
2	Silver	36	0.056	3.69
3	Gold	10	0.38	2.61
4	Water	0	1.33	0

4. P polarization

Fig. S2 shows that the directional Raman scattering was almost completely p-polarized. The polarization factors (the intensity ratio of the p-polarized to s-polarized signal) of the emitted SPCR signals from MG were determined to be 9.34 (1173 cm^{-1}), 9.88 (1368 cm^{-1}), 8.12 (1397 cm^{-1}), and 7.83 (1617 cm^{-1}), separately. The p-polarized emission observed in the experiments concurs with the theory of SPCE,¹ where such emission is only triggered at θ_{sp} , thereby resulting in predominantly p-polarized signature-based plasmon-coupled emission signals. This indicates that the p-polarized directional Raman signal through a prism is not a virtue of the transmission of SERS, but rather originates from the coupling between SERS and PSPs, and that this coupling is the root of directional emission of the SPCR signal.

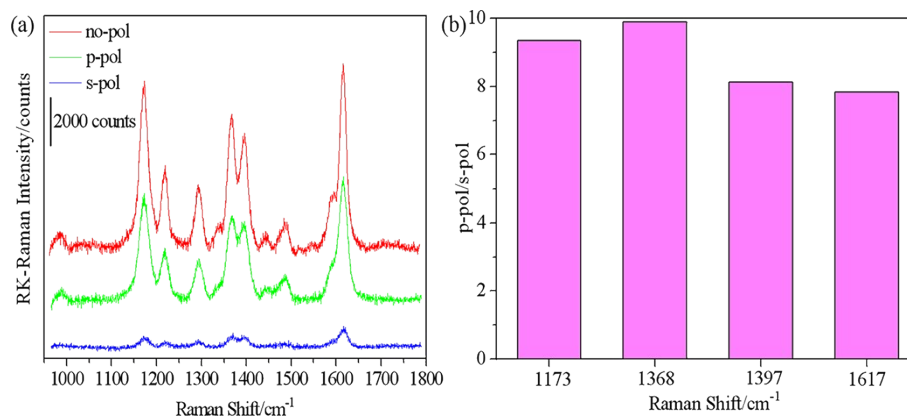


Fig. S2 (a) SPCR spectra of MG without (no-pol) and with p-polarization (p-pol) or s-polarization (s-pol). (b) The polarization factor of the SPCR signal.

5. LSP effect on the coupling efficiency

Fig. S3 shows the SEM images of bimetallic films with different surface coverage of Au NPs. As the concentrations of colloidal Au NPs added increased, the coverage of Au NPs increased from 0.16 to 0.41, 1.34, 2.26 and 3.7 $\text{NP}/\mu\text{m}^2$.

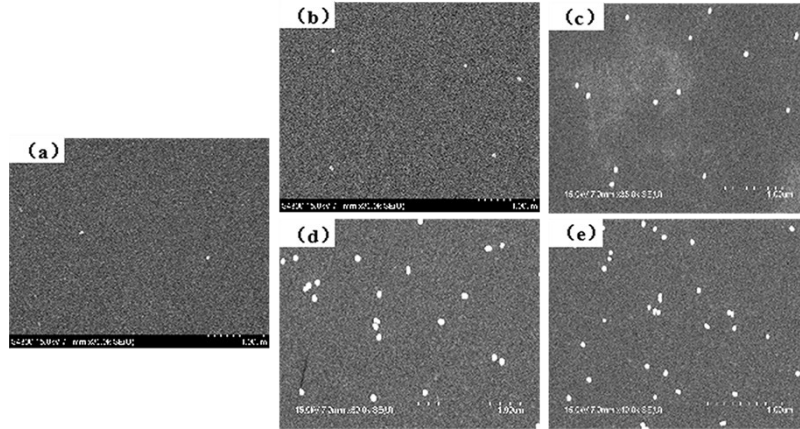


Fig. S3 (a) ~ (e) The scanning electron microscope images of bimetallic film with different Au NP coverages.

The SPCR signals corresponding to four main peaks of MG versus the surface coverage of Au NPs are plotted in Fig. S4. Localized surface plasmons (LSPs) act as enhancers for SERS and competitors to coupling efficiency between PSPs and SERS. The coupling efficiency increased as the coverage of Au NPs increased. Due to the formation of more active “hot spots”, nanoparticle-induced LSPs ensured that extremely strong coupling to PSPs was achieved to generate intense SPCE. This is because the hybridized field composed of the excited LSP and PSP was confined within a narrow gap between the nanoparticles and the thin film.^{2, 3} On the other hand, larger coverage of Au NPs on the smooth metal film would cause broadening and higher reflectance in the SPR curve. Similarly, in SPCR, excessive LSPs would disturb the coupling efficiency between the LSPs on nanoparticles and PSPs on metal film.³⁻⁵ The variation in SPCR intensity was consistent with the above theory and initially increased as the coverage of Au NPs increased, reached a maximum and then decreased.

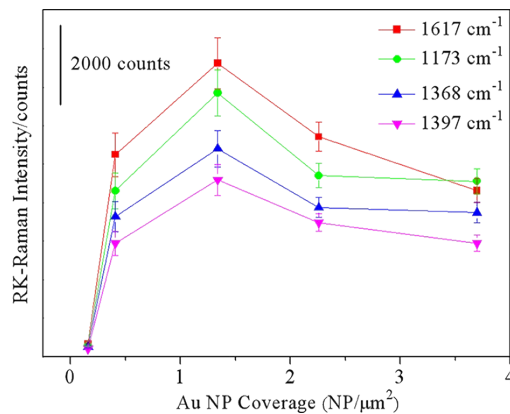


Fig. S4 The SPCR intensity of four main Raman bands of MG under different Au NP coverages.

6. The normal Raman spectrum of malachite green

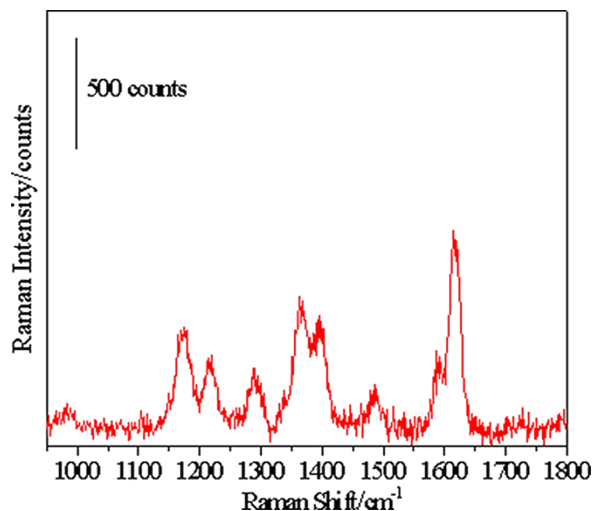


Fig. S5 The normal Raman spectrum of solid malachite green.

Fig. S5 shows the normal Raman spectra of malachite green, the ratios of $I_{1173\text{ cm}^{-1}}$, $I_{1362\text{ cm}^{-1}}$, $I_{1398\text{ cm}^{-1}}$, and $I_{1615\text{ cm}^{-1}}$ to $I_{1219\text{ cm}^{-1}}$ are 1.47, 1.45, 1.24, and 2.11, separately.

1. S.-H. Cao, W.-P. Cai, Q. Liu and Y.-Q. Li, in *Annual Review of Analytical Chemistry*, 2012, **5**, 317-336.
2. S.-H. Cao, W.-P. Cai, Q. Liu, K.-X. Xie, Y.-H. Weng, S.-X. Huo, Z.-Q. Tian and Y.-Q. Li, *Journal of the American Chemical Society*, 2014, **136**, 6802-6805.
3. M. H. Chowdhury, K. Ray, C. D. Geddes and J. R. Lakowicz, *Chemical Physics Letters*, 2008, **452**, 162-167.
4. L. A. Lyon, D. J. Pena and M. J. Natan, *Journal of Physical Chemistry B*, 1999, **103**, 5826-5831.
5. L. He, E. A. Smith, M. J. Natan and C. D. Keating, *Journal of Physical Chemistry B*, 2004, **108**, 10973-10980.